Biosorption of Cesium-134 from Aqueous Solutions using Immobilized Marine Algae: Equilibrium and kinetics

H. A. Omar [1]; A.S. Abdel-Razek [2]; M.S. Sayed [2]

[1]Radiation Protection Dept. - Nuclear Research Center - Atomic Energy Authority, Cairo, Egypt.
[2]Radiation Protection Dept. - Hot Laboratories Center- Atomic Energy Authority, Cairo, Egypt.
hodaatom@yahoo.com alasayabdelr@yahoo.com .

Abstract: Marine green algae *Enteromorpha torta* (Wulfen) J. Agardh (Chlorophyta: Ulvales) collected from western Alexandria coast was investigated for the removal of ^{134}Cs from aqueous solutions. Different dry weights of *E. torta* (0.2, 0.15, 0.1, 0.05 and 0.025g) were immobilized using 10 ml of 4% calcium alginate. The equilibrium sorption studies for ^{134}Cs were done using 2g (50 beads) of control Ca-alginate (CA) and immobilized algal biomass (IAB) beads. The experimental data have been analyzed using Langmuir, Freundlich and Dubinin-Radushkevich isotherms. The results showed that the maximum capacity was 4.32, 3.77, 3.51, 4.6, 10.55 and 12.6 mmol/g dry weights for control, 0.2, 0.15, 0.1, .05 and 0.025g of *E. torta*, respectively. The mean free energy was 18.9, 19.03, 21.13, 22.71, 23.47 and 23.59 KJmol^{-1} for the same samples. Moreover, sorption kinetics was performed and it was observed that the equilibrium reached in three hours, which could be described by pseudo-first-order and pseudo-second-order kinetic models. The maximum biosorption of ^{134}Cs was investigated at pH 7 for all sorbents. Column experiments were also carried out to investigate the capacity of IAB beads for cesium-134.
[H. A. Omar; A.S. Abdel-Razek; M.S. Sayed. Biosorption of Cesium-134 from Aqueous Solutions using Immobilized Marine Algae: Equilibrium and kinetics. Nature and Science 2010;8(11):140-147] (ISSN: 1545-0740).

Key words: biosorption; green algae; calcium alginate; ^{134}Cs; kinetics.

1. Introduction:

Waterways represent an important group of natural resources, habitats, and living organisms that need protection from various stress factors including radionuclide releases. Marine and freshwaters can receive low-level radioactive liquid wastes discharged from nuclear facilities under normal operating conditions or may be accidentally contaminated such as occurred during the Chernobyl accident (Adam, 2003). Biosorption has provided an alternative treatment of industrial effluents from that of the traditional physico-chemical methods (Gupta, 2008b). The biological materials that have been investigated for the uptake of toxic metals include bacteria, fungi, yeast and algae (Palmieri, 2002; Bishnoi, 2007; Congeevaram, 2007; Ozturk, 2007). Algae play a key role in controlling radioactive contamination of marine and freshwater ecosystems, as a point of entry of pollutants within trophic nets and because of their accumulation of radionuclides very quickly to a high level, cheap availability, relatively high surface area and high uptake capacities (Figuera, 2000; Davis, 2003; Gupta, 2008a). Algal biomass can be used for biosorption process in live or dead form. However, in practical applications, the use of nonliving biomass is more practical and advantageous because living biomass cells often require the addition of fermentation media which increases the biological oxygen demand or chemical oxygen demanded in the effluent. In addition, non-living biomass is not affected by the toxicity of the metal ions; they can be subjected to different chemical and physical treatment techniques to enhance their performance (Gong, 2005). The cell wall of algae consists of chitin, lipids, polysaccharides and proteins. These macromolecules provide different functional groups, such as thioether, carboxyl, imidazole, hydroxyl, carbonyl, phosphate, phenolic, etc., which can form coordination complexes with metal ions (Figuera, 2000). Application of immobilization technology to algal wastewater treatment provides more flexibility when compared with conventional suspension systems. Moreover, accelerated reaction rates due to increased cell density, increased cell wall permeability, no washout of cells, ease of separation and better operational stability are the additional advantages of immobilized cells over their free-living counterparts (Mallick**,** 2002).

The aim of this paper is to determine the effect of the basic parameters such as pH, contact time and initial metal concentration on the cesium-134 biosorption by control Ca-alginate (CA) and immobilized algal biomass (IAB) beads as batch and column technique.

2. Materials and Methods:

2.1 Chemicals and reagents

All chemicals used were of analytical reagent grade (BDH Company). Cesium chloride solutions

were prepared by dissolving appropriate quantities of cesium chloride salt. Deionized water was used throughout all experiments. The pH was adjusted by appropriate concentration of NaOH or HCl.

2.2. Preparation of biomass

The marine algal species *Enteromorpha torta* (E.Torta) (Mertens) Reinbold (Keegan, 1986) was collected from the Mediterranean Sea at western Alexandria coast. The collected biomasses were washed with excess tap water and finally with distilled water to remove salt and particulate materials from its surface, then oven-dried at 60°C for 24 h. The dried biomasses were ground, sieved to particle size ranged from 0.25µm to 0.3µm and then stored in a dessicator at lab temperature for use.

2.3. Preparation of biosorbent beads

The control Ca-alginate (CA) beads were prepared by injecting 10 ml of 4% Ca-alginate gel into 2% $CaCl_2$ solution, while the immobilized algal biomass (IAB) beads were prepared by mixing the desired weight of dried algal biomass with 10 ml of 4% Ca-alginate gel thoroughly, then injected into 2% $CaCl_2$ solution. The formed beads of (CA) or (IAB) were left in $CaCl_2$ solution for one hour, and then washed twice with bi-distilled water. 10 ml of calcium alginate gel gives about 300 beads of (CA) or (IAB) having diameter 2.5-3.0 mm. The obtained beads were kept in refrigerator at 4°C for use.

2.4. Biosorption experiments

2.4.1. Batch studies

The pH values of the aqueous solutions were measured using pH meter model (Orion Research digital ion analyzer 501). In order to adjust the environmental parameters, 0.1mol l^{-1} NaCl was used to control the ionic strength and hexamethylene tetramine solution (20 %, w/w) was used for keeping proton balance. The pH of each solution was adjusted with 0.1mol l^{-1} NaOH or HCl. Unless otherwise stated, 50 beads (2 g) of CA or IAB beads were placed in a 50 ml Erlenmeyer flask and treated with 20 ml of 10^{-5} M cesium solution, traced with the radioactive isotope. Solution samples were taken for ^{134}Cs activity determination using NaI scintillation crystal connected to a ACE™ multichannel analyzer (ORTEC). The uptake percent (U%) of ^{134}Cs was calculated from the following equation:

$$U\% = (A_o\text{-}A)/A_o X100 \qquad (1)$$

Where A_o and A are the activities expressed in counts per minute of 1 ml solution for the radioisotope before and after contacting with the biosorbent. The amount of cesium ion adsorbed at equilibrium, q_e (mmol g^{-1}), which presents the metal uptake on the sorbent, was calculated from the difference in metal concentration in the aqueous phase before and after biosorption, according to the following equation:

$$q_e = U\% \text{ X } C_o \text{ X } V/m \qquad (2)$$

where; C_o is the initial metal ion concentration in (mmol/l), V and m are the volume of aqueous solution in (l) and the dry weight of biosorbent in (g), respectively. Each experiment was repeated three times, and the results were given as averages. The dry weight of 50 beads of (CA) was 0.06 g , while that of 50 beads of 0.2, 0.15, 0.1, 0.05 and 0.025g (IAB) were 0.093, 0.085, 0.077, 0.068 and 0.064 g , respectively.

2.4.2. Column studies

Sorption experiments were carried out in a glass column (1cm internal diameter and 10 cm height). The column was packed with 2 grams of (IAB) beads at bed depth 2 cm. The pH of ^{134}Cs solution was adjusted to 7. The traced cesium ion solution with fixed concentration of $1X10^{-5}$M was fed by peristaltic pump through the column at different flow rates; 5, 10 and 15 ml/min. Samples were collected at regular time intervals and counted by using NaI scintillation crystal connected to a ACE™ multichannel analyzer (ORTEC).

3 Results and Discussion

3.1. Effect of pH

The effect of pH on metal biosorption has been studied, and the results indicated that the pH value of solution could significantly influence biosorption (Fourest, 1994; Liping, 2008). The influence of initial pH on the adsorption characteristics of ^{134}Cs using Ca-alginate (CA) and immobilized algal biomass (IAB) beads is shown in Fig. (1). A trend of increasing metal ion binding with increasing pH could be observed for all sorbents at pH values above 2.5. The optimal removal efficiencies of ^{134}Cs were observed for the pH range 6.5-7.5. The cell wall of algae contains a large number of surface functional groups, in which carboxyl is generally the most abundant acidic functional group according to (Figuera, 2000). At low pH, cell wall ligands are closely associated with the excess of hydronium ions (H_3O^+) and hence the sorption of positive Cs ions to the ligands will be restricted. With increasing pH, (H_3O^+) decreased and carboxyl groups will be exposed to attraction with the positive charges Cs ions and hence an increases in biosorption onto the cell surface was observed in agreement with (Matheickal, 1999).

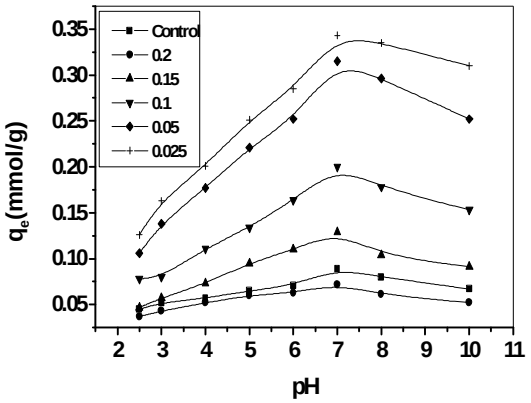

Fig. (1): Effect of pH values on biosorption of ^{134}Cs onto control CA and IAB beads.

3.2. The effect of immobilized weight

The weight of biomass to be immobilized is an important parameter in the immobilization process (Abdel-Hameed, 2006). For constant volume of Ca-alginate gel (10 ml), different dry weights (0.2, 0.15, 0.1, 0.05 and 0.025g) of algal biomass were mixed. The effect of immobilized biomass on the biosorption of ^{134}Cs was studied at room temperature and pH 7.0, with initial cesium concentration of 10^{-5}M Fig.(2). It is apparent that the removal of ^{134}Cs increased as the immobilized weight decreased. Thus the optimum weight to be immobilized in 10 ml Ca-alginate gel was 0.025 g. This could be explained by the interaction between the active groups of the excess algal biomass and that of the gel, resulting in decreasing the free and available active sites on both the immobilized algal biomass and the gel.

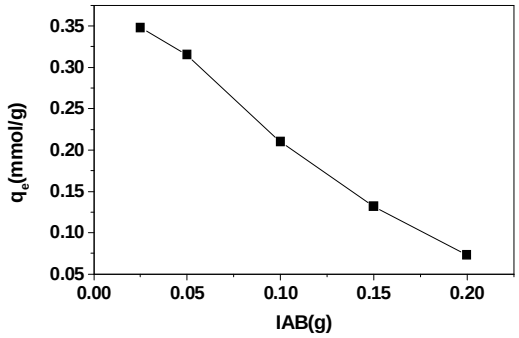

Fig. (2): Effect of IAB weight on the removal of ^{134}Cs

3.3 Effect of contact time

Figure (3) shows plots of the amount of ^{134}Cs sorbed onto different beads, at initial concentration of 10^{-5}M and at room temperature (25±1°C), as a function of contact time. There was high initial rate of removal within the first 60 minutes of contact followed by a slower subsequent removal rate that gradually approached an equilibrium condition in about three hours for all beads. These changes in metal uptake may be due to the fact that, initially, all adsorbent sites were vacant and the solute concentration was high. After that period, only a very low increase in the metal uptake was observed because, there were few active sites on the biosorbent beads.

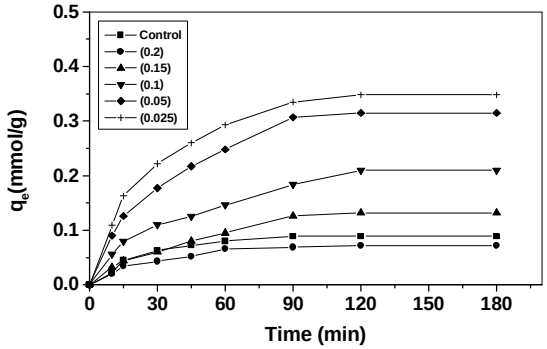

Fig. (3): Amount of adsorbed ^{134}Cs onto control CA and IAB beads at different contact times.

3.4 Sorption kinetics

The study of adsorption kinetics describes the solute uptake rate and evidently this rate controls the residence time of adsorbent at the solid-solution interface. The kinetics of ^{134}Cs adsorption on CA and IAB beads were analyzed using pseudo first order (Nuhoglu, 2009), pseudo second order (Ho, 2004) and intraparticle diffusion kinetic models (Huh, 2000). The conformity between experimental data and the model predicted values was expressed by the correlation coefficients (R^2). A relatively high R^2 value (R^2 values close or equal to 1) indicates that the model successfully describes the kinetics of the adsorption.

3.4.1 Pseudo-first-order model

The behavior of the batch sorption process of ^{134}Cs was analyzed using Lagergren first order kinetics model (Nuhoglu, 2009). The Lagergren first order model is given by equation:

$$\log (q_e-q_t) = \log q_e - K_1/2.303\ t \qquad (3)$$

where; q_e and q_t are concentration (mmol/g) of ^{134}Cs onto the biosorbent at equilibrium and at time t, respectively. The slope and intercept of the plots of log (q_e-q_t) versus t, as shown in Fig (4), were used in calculating the pseudo first order rate constant (min^{-1}) and the theoretical equilibrium sorption capacities (q_e), respectively. The values of K_1, q_e and the linear correlation coefficients (R^2) were presented in Table (1). As can be seen from Table (1), linear correlation coefficients of the plots are not good for all biosorbent samples except control CA and IAB 0.025g. So, it

could suggest that the sorption of ^{134}Cs onto other biosorbent samples is not a first order reaction.

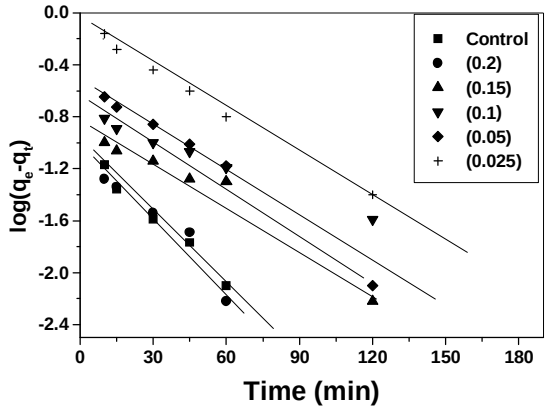

Fig. (4): Lagergren Kinetic model for adsorption of ^{134}Cs onto control CA and IAB beads.

3.4.2 Pseudo second-order model

A pseudo second-order model was also used to describe the kinetics of ^{134}Cs sorption onto the biosorbents. This model is expressed as:

$$t/q_t = 1/K_2q_e^2 + 1/q_e \; t \qquad (4)$$

where; K_2 is the rate constant of pseudo second-order equation (mmol/g. min). The kinetic plots of t/q_t versus t for ^{134}Cs sorption onto different beads are represented in Fig. (5). The relations are linear and the values of the correlation coefficient (R^2) suggest a strong relationship between the parameters. The product $K_2q_e^2$ is the initial sorption rate represented as $h = k_2q_e^2$. The kinetics parameters of this model were calculated from the slope and intercept of the linear plots and are given in Table (1). The correlation coefficients were higher compared to the results obtained from the first –order kinetic model. So, it is possible to suggest that the sorption of ^{134}Cs followed the pseudo second-order kinetics model.

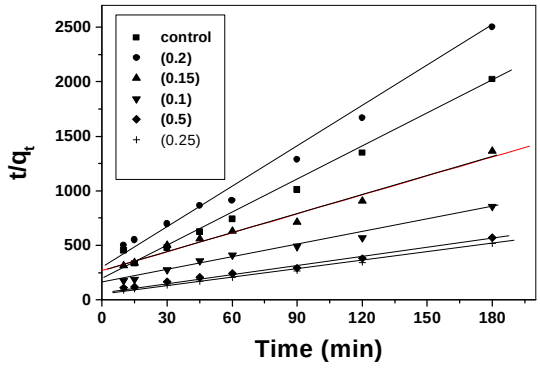

Fig. (5): Pseudo-second order kinetic plots for ^{134}Cs sorption onto control CA and IAB beads.

Table (1): Calculated parameters of the pseudo-first order and pseudo-second order kinetic models for ^{134}Cs sorption onto control CA and IAB beads.

		Pseudo First Order Parameters			Pseudo Second Order Parameters				
		K_1 min^{-1}	$q_{e\ calc.}$ (mmol/g)	R^2	K_2 mmol . g^{-1} min^{-1}	h	$q_{e\ calc.}$ (mmol/g)	R^2	$q_{e\ exp.}$ (mmol/g)
Control (CA) Beads		0.0396	0.0897	0.9911	0.424	0.0046	0.104	0.9921	0.089
(IAB) Beads	**(0.2)**	0.0405	0.084	0.9815	0.406	0.0031	0.087	0.9943	0.072
	(0.15)	0.0328	0.173	0.9499	0.124	0.0037	0.173	0.9899	0.132
	(0.1)	0.0211	0.195	0.9823	0.097	0.0066	0.261	0.9933	0.21
	(0.05)	0.0389	0.414	0.9563	0.085	0.0123	0.381	0.9960	0.315
	(0.025)	0.0347	0.355	0.9884	0.101	0.0167	0.406	0.9981	0.348

3.4.3 Morris-Weber model

The kinetics of sorption of ^{134}Cs onto biosorbent samples was also evaluated by Morris-Weber kinetic model (Huh, 2000); which is expressed as:

$$q_e = K_d.t^{1/2} \qquad (5)$$

where; q_e is the concentration of sorbed ion (mmol/g) at time t, and K_d is the rate constant for intra-particle transport (mmol/g $min^{1/2}$). According to this model, a plot of q_e versus $t^{1/2}$ could predict the sorption mechanism of ^{134}Cs. If a straight line (passing through the origin) is obtained, therefore, sorption of ^{134}Cs onto control CA and IAB beads follows a diffusion mechanism. The slope of the linear plot indicates the rate constant of intra-particle transport (K_d). The results are shown in Fig. (6) and tabulated in Table (2).

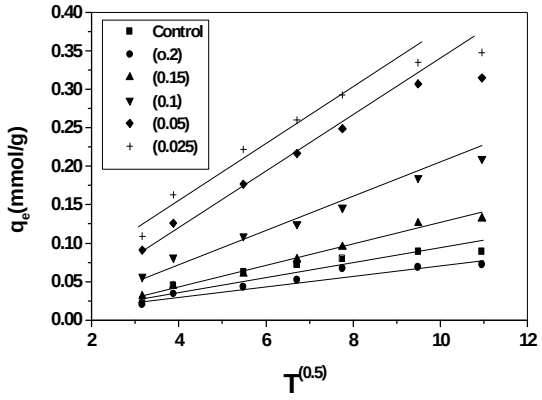

Fig. (6): Morris Weber Kinetic plots for sorption of ^{134}Cs onto control CA and IAB beads.

Table (2): Morris-Weber kinetic model for ^{134}Cs sorption onto biosorbent beads.

		K_d	R^2
Control (CA) Beads		0.0081	0.9337
(IAB) Beads	**(0.2)**	0.0066	0.95791
	(0.15)	0.0136	0.99347
	(0.1)	0.01913	0.99692
	(0.05)	0.0298	0.98913
	(0.025)	0.0302	0.9884

3.5 Adsorption isotherms

The sorption isotherms were studied using different concentrations of CsCl ranged from 10^{-5} to 10^{-3}M. The variation of sorption with the concentration of sorbate was fitted to different sorption isotherms, namely Langmuir, Freundlich and Dubinin–Radushkevich (D–R) to evaluate the sorption capacities of the sorbents.

3.5.1 Langmuir isotherm

The Langmuir sorption isotherm was tested in the following linearized form:

$$C_e/q_e = 1/Q_0b + 1/Q_0 \, . \, C_e \qquad (6)$$

where; C_e and q_e are concentration of sorbate in solution and at the sorbent surface at equilibrium, and Q_0 and b are characteristic constants related to adsorption capacity and energy of adsorption, respectively. In Fig. (7), C_e/q_e is plotted against C_e for ^{134}Cs. The slope of this linear plot gives the value of Q_0 whereas from the intercept the value of b was computed Table (3). The Langmuir isotherm assumes that ions are sorbed on definite sites that are monoenergetic on the sorbent surface and each site can accommodate only one molecule or ion. The sorbed ions cannot migrate across the surface or interact with neighboring molecules (Langmuir, 1918).

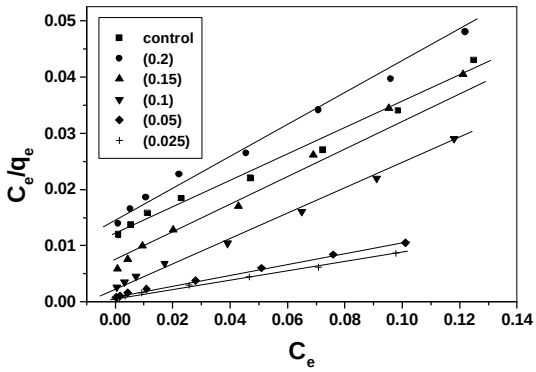

Fig. (7): Langmuir adsorption isotherm of ^{134}Cs sorption onto control CA and IAB beads.

3.5.2 Freundlich isotherm

The Freundlich sorption isotherm can be expressed by:

$$\log q_e = \log K_f + 1/n \ \log C_e \qquad (7)$$

where; K_f and n are Freundlich constants characteristic of adsorption capacity and adsorption intensity, respectively. The plot of log q_e versus log C_e will give a straight line, if it follows Freundlich sorption isotherm Fig. (8). The slope and intercept of the linear Freundlich equation are equivalent to 1/n and log K_f, respectively. The Freundlich sorption isotherm encompasses the heterogeneity of the surface and exponential distribution of sites and their energies (Freundlich, 1939). The characteristic Freundlich constant 1/n should be less than unity. The steep slope of 1/n close to unity indicates high sorptive capacity at higher equilibrium concentrations. The Freundlich parameters are given also in Table (3).

3.5.3. Dubinin–Radushkevich (D–R)

The sorption data for the metal ion was tested on another isotherm, namely D–R in the following form (Dubinin, 1947);

$$\ln q_e = \ln q_m - \beta\varepsilon^2 \qquad (8)$$

where; q_e and q_m are sorbed concentration and maximum sorption capacity at the sorbent surface and, β is a constant related to sorption energy, and ε is Polanyi potential which is equal to:

$$\varepsilon = RT \ln (1 + 1/C_e) \qquad (9)$$

where; R is the universal gas constant in $kJmol^{-1}$, T is the absorbents temperature in Kelvin and C_e is the equilibrium concentration of sorbate in solution. When lnq_e is plotted against ε^2, a straight line may be obtained if the sorption data follow the D–R isotherm. The D–R isotherms are shown in Fig. (9).

The slope of the linear plot gives the value of β and the intercept yields the value of maximum sorption capacity, q_m, The value of β can be correlated to sorption free energy (E) using the following relationship **(**Hobson, 1969):

$$E = 1/ (2\beta)^{1/2} \qquad (10)$$

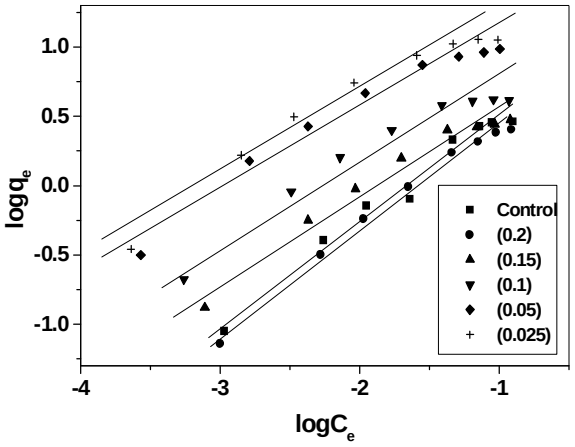

Fig. (8): Freundlich adsorption isotherm of ^{134}Cs sorption onto control CA and IAB beads.

Table (3): Langmuir, Freundlich and D–R parameters for different biosorbent beads.

		Langmuir isotherm parameters			Freundlish isotherm parameters			D-R isotherm parameters		
		Q_0 (mmol/g)	B	R^2	1/n	K_f mmol/g	R^2	E (KJ mol^{-})	q_m (mmol/g)	R^2
Control (CA) Beads		4.322	19.1	0.9929	0.74945	3.45	0.9887	18.9	4.54	0.9976
(IAB) Beads	**(0.2)**	3.77	17.58	0.9964	0.74667	3.24	0.9939	19.03	3.73	0.9973
	(0.15)	3.51	44.87	0.9977	0.61315	3.15	0.9814	21.13	4.42	0.9983
	(0.1)	4.61	83.11	0.9983	0.54951	3.55	0.9708	22.71	6.37	0.9969
	(0.05)	10.55	86.96	0.9988	0.56089	5.26	0.9788	23.47	14.14	0.9991
	(0.025)	12.6	102.01	0.9991	0.56493	5.87	0.9762	23.59	17.63	0.9988

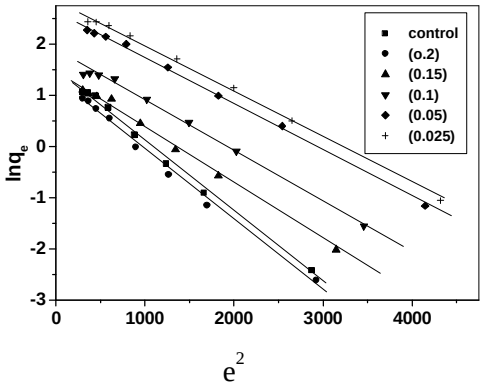

Fig. (9): D-R isotherm for ^{134}Cs sorption onto control CA and IAB beads.

The corresponding values of β, q_m and E computed for ^{134}Cs are listed in Table (3). The D–R isotherm is powerful and simple in concept and applications and can be employed from trace to saturation concentrations. Polanyi potential, ε is the work required to remove a molecule or ion away from its location in the ‘‘sorption space’’. The D–R isotherm assumes a fixed volume or ‘‘sorption space’’ close to the sorbent surface where sorption takes place. It describes heterogeneity of sorption energies within this space, independent of temperature. If E is in the range of 8-16 KJ/mol, sorption is governed by ion exchange. In case of E< 8.0 KJ/mol, physical forces may affect the sorption mechanism and If E> 16.0 KJ/mol, chemical forces may affect the sorption mechanism. The sorption energy, E, for ^{134}Cs was >16 kJ/mol, this indicated that the biosorption process of ^{134}Cs by control CA or IAB beads is chemical process.

3.6. Column techniques

The time for breakthrough appearance and the shape of the breakthrough curve are very important characteristics for determining the operation and the dynamic response of an adsorption column. The breakthrough curves show the loading behavior of metal to be removed from solution in a fixed bed and is usually expressed in terms of adsorbed metal concentration (C_{ad}), inlet metal concentration (C_0), outlet metal concentration (C_t) or normalized concentration defined as the ratio of effluent metal concentration to inlet metal concentration (C_t/C_0) as a function of time or volume of effluent for a given bed height (Diniz, 2008).

Break-through capacity $q_e(0.5)=V(50\%)XC_o/m$ (11)

3.6.1. Effect of flow rate

The influence of flow rate on the biosorption of ^{134}Cs by IAB was investigated through keeping initial Cs ion concentration 10^{-5} M, 2 gm of adsorbent and bed height (2 cm) constant and varying the flow rate from 5 to 15ml/min. In contrast to bed height results, the column performed well at lowest flow rate. Initially the adsorption was very rapid at lower flow rate probably associated with the availability of reaction sites able to capture metal ions around or inside the cells. In the next stage of the process due to the gradual occupancy of these sites, the uptake becomes less effective. The breakthrough curve becomes steeper when the flow rate is increased with the break point time and adsorbed ion concentration decreases. The probable reason behind this is that when the residence time of the solute in the column is not long enough for adsorption equilibrium to be reached at that flow rate, the cesium solution leaves the column before equilibrium. Thus, the contact time of cesium ions with IAB beads is very short at higher flow rate, causing a reduction in removal efficiency (Goel, 2005).

An earlier breakthrough and exhaustion time were observed in the profile, when the flow rate was increased to 15 ml/min. The flow rate also strongly influenced the cesium uptake capacity of IAB beads as 0.703, 0.603 and 0.44 mg/g, were recorded at 5, 10 and 15 ml/min, respectively. Breakthrough curves, C_t/C_0 against volume throughput is shown in Fig. (10).

4. Conclusion:

The immobilized algal biomass (IAB) enhances the adsorption capacity of Ca-alginate beads especially in case of low weight (0.025g/10ml gel). The pH of the adsorbate (^{134}Cs) solution and the weight of the immobilized algal biomass are controlling factors in the adsorption process. The different kinetic models used in analyzing the experimental data indicated that pseudo-second order sorption mechanism is predominant and the adsorption process is a chemical process. Comparing the regression coefficient (R^2) for the three isotherms, it was concluded that Dubinin–Radushkevich (D–R) is the best with average R^2 value of 0.998 followed by Langmuir with average R^2 0.9947 then Freundlich with average R^2 0.9816.

The maximum adsorption capacity of ^{134}Cs were; 4.32, 3.77, 3.51, 4.61, 10.55 and 12.6 mmol/g dry weight for control (CA) beads and 0.2, 0.15, 0.1, .05, 0.025g (IAB) beads, respectively. The fixed bed column study showed that the flow rate strongly influenced ^{134}Cs uptake capacity of IAB beads, where the capacity for column of 2 cm bed height, 2 g adsorbent weight and at Cs ion concentration 10^{-5} M were; 0.703, 0.603 and 0.44 mg/g, at flow rates 5, 10 and 15 ml/min, respectively.

The dry weight of CA beads represents 3% of the wet weight, while the dry weight of (0.2g/10ml gel) IAB beads represent 4.5% of the wet weight. This means that we have a volume reduction ranged from 97 – 95.5%, which is a great advantage and major concept in the treatment of radioactive waste effluents. The present study indicated that immobilized *E. torta* could be used for the removal of ^{134}Cs from aqueous solutions.

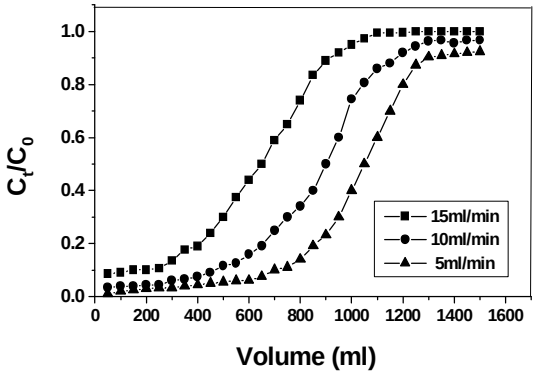

Fig. (10): Breakthrough curves of ^{134}Cs sorption onto IAB beads at different flow rates.

Corresponding author
H. A. Omar
[1]Radiation Protection Dept. - Nuclear Research Center - Atomic Energy Authority, Cairo, Egypt.
hodaatom@yahoo.com

5. References:

1. Abdel-Hameed MS. Continuous removal and recovery of lead by alginate beads, free and alginate-immobilized *Chlorella vulgaris*. African J Biotechnol 2006; 5(19):1819–1823.

2. Adam C, Garnier-Laplace J. Bioaccumulation of silver-110m, cobalt-60, cesium-137 and manganese-54 by the freashwater algae *Scenedesmus obliquus* and *Cyclotella meneghiana* and by suspended matter collected during a summer bloom event. Limnol Oceanogr 2003; 48(6): 2303- 2323.
3. Bishnoi NR, Kumar R, Kumar S, Rani S. Biosorption of Cr(III) from aqueous solution using algal biomass *Spirogyra* sp. J Hazard Mater 2007; 145: 142-147.
4. Congeevaram S, Dhanarani S, Park J, Dexilin M, Thamaraiselvi K. Biosorption of chromium and nickel by heavy metal resistant fungal and bacterial isolates. J Hazard Mater 2007; 146: 270-277.
5. Davis TA, Volesky B, Mucci A. A review of the biochemistry of heavy metal biosorption by brown algae. Water Res 2003; 37(18): 4311-4390.
6. Diniz V, Weber ME, Volesky B, Naja G. Column biosorption of lanthanum and europium by *Sargassum*. Water Res 2008; 42:363-371.
7. Dubinin MM, Radushkevich LV. Equation of the characteristic curve of activated charcoal. Chem Zentr 1947; 1(1): p 875.
8. Figuera MW, Volesky B, Ciminelli VS, Roddick FA. Biosorption of metals in brown seaweed biomass. Water Res 2000; 34 (1):196-204.
9. Fourest E, Canal C, Roux JC. Improvement of heavy metal biosorption by mycelial dead biomasses (*Rhizopus arrhizus*, *Mucor miehei* and *Penicillium chrysogenum*): pH control and cationic activation. Fems Microbiol Rev 1994; 14: 325–332.
10. Freundlich H, Hellen W. The adsorption of Cis- and Trans-Azobenzen. J Amer Chem Soc 1939; 61(8): 2228-2230.
11. Goel J, Kadirvelu K, Rajagopal C, Garg VK. Removal of lead by adsorption using treated granular activated carbon: Batch and column studies. J Hazard Mater 2005; B125: 211-220.
12. Gong R, Ding Y D, Liu H, Chen Q, Liu Z. Lead biosorption and desorption by intact and pretreated *Spirulina maxima* Biomass. Chemosphere 2005; 58(1): 125–130.
13. Gupta VK, Rastogi, A. Biosorption of lead from aqueous solutions by green algae *Spirogyra* species: Kinetics and equilibrium studies. J Hazard Mater 2008a; 152: 497-414.
14. Gupta VK, Rastogi A. Sorption and desorption studies of chromium (VI) from nonviable cyanobacterium *Nostoc miscorum* biomass. J Hazard Mater 2008b; 154: 347-354.
15. Ho YS. Comment on Cadmium removal from aqueous solutions by chitin: kinetic and equilibrium studies. Water Res 2004; 38(12): 2962-2964.
16. Hobson JP. Physical adsorption isotherms extending from ultrahigh vacuum to vapor pressure. J Phy Chem 1969; 73: 2720-2727.
17. Huh JK, Song D-I, Jeon Y-W. Sorption of phenol and alkylphenol from aqueous solution onto organically modified montmorillonite and application of dual-mode sorption model. Separ Sci Technol 2000; 35(2): 243-259.
18. Keegan BF, Mercer JP. An oceanographical survey of Killary Harbour on the west coast of Ireland. Proceedings of the Royal Irish Academy 1986; 86B: 1-70.
19. Langmuir I. The adsorption of gases on plane surfaces of glass, mica and platinum. J Amer Chem Soc 1918; 40(9): 1361-1403.
20. Liping D, Xiaobin Z, Yingying S, Hua S, Xinting W. Biosorption and desorption of Cd^{2+} from wastewater by dehydrated shreds of *Cladophora fascicularis.* Chinese Journal of Oceanology and Limnology 2008; 26 (1): 45-49.
21. Mallick N. Biotechnological potential of immobilized algae for wastewater N, P and metal removal: A review. BioMetals 2002; 15: 377–390.
22. Matheickal JT, Yu QM, Woodburn GM. Biosorption of Cadmium(II) from aqueous solutions by pre-treated biomass of marine alga *Durvillaea potatorum*. Water Res 1999; 33: 335–342.
23. Nuhoglu Y, Malkoc E. Thermodynamic and kinetic studies for environmentaly friendly Ni(II) biosorption using waste pomace of olive oil factory. Biores Technol 2009; 100: 2375–2380
24. Ozturk A. Removal of nickel from aqueous solution by the bacterium *Bacillus thuringiensis*. J Hazard Mater 2007; 147: 518-523.
25. Palmieri MC, Volesky B, Garcia O. Biosorption of lanthanum using *Sargassum fluitans* in batch system. Hydrometallurgy 2002; 67: 31-36.

9/25/2010